Zinc is a determinant of the cytotoxicity of Ziram, a dithiocarbamate fungicide, in rat thymic lymphocytes: Possible environmental risk

Yumiko Kanemoto-Kataoka [#], Tomohiro M. Oyama [##], Hitoshi Ishibashi [###], Yasuo Oyama *

Faculty of Bioscience and Bioindustry, Tokushima University, Tokushima 770-8513, Japan

Present address:

[#] Bayer Yakuhin, Ltd., Osaka 530-0001, Japan

[##] Medical Co. LTA Clinical Pharmacology Research Units, Kumamoto 861-4157, Japan

[###] Kitasato University, Kanagawa 252-0373, Japan

*Corresponding author: Yasuo Oyama, Ph.D.

E-mail: oyamay@tokushima-u.ac.jp; Tel: 81-88-656-7256

Abstract

Ziram, one of dithiocarbamate fungicides, is widely applied to agriculture because the agent protects various crops from fungal infections. Risks of dithiocarbamate biocide use are concerned. It was previously reported that Ziram increased the intracellular concentration of Zn^{2+}. Therefore, we cytometrically studied the mechanism of Zn^{2+}-dependent lethal actions of Ziram on rat lymphocytes under environmentally relevant Zn^{2+} levels. Membrane and cellular parameters of rat lymphocytes were estimated by flow-cytometric techniques with appropriate fluorescent probes. The Ziram-induced increase in cell lethality was completely attenuated by Zn^{2+} chelators. A significant raise of cell lethality was found on the simultaneous application of Ziram at a sublethal concentration and $ZnCl_2$. The combination of Ziram and $ZnCl_2$ increased the cellular superoxide anion content and decreased the cellular GSH content, which possibly caused the increase in cell lethality. The zinc concentrations under present experimental conditions were comparable to the environmentally relevant concentrations found in rivers. Therefore, the environmental level of zinc may be critical in estimating the toxicity of Ziram to wild animals.

Keywords:

Fungicide

Dithiocarbamate

Lymphocytes

Cytotoxicity

Zinc

1. Introduction

Ziram, one of dithiocarbamate fungicides (Fig. 1), is employed to protect crops from fungal infections in agriculture [1–3]. The use of dithiocarbamate biocide has raised increasing concerns regarding its environmental and health risks [2,3]. Experiments were performed to evaluate the cellular toxicity of Ziram in rat hippocampal astrocytes [4]. Ziram accelerated lipid peroxidation and lowered the cellular glutathione (GSH) content. The oxidation of thiols to disulfides resulted in Zn^{2+} release from thiols of protein and nonprotein [5]. Ziram raised $[Zn^{2+}]_i$, but not $[Ca^{2+}]_i$, and increased the living cells that were positive to annexin V [6]. Therefore, we hypothesize that Ziram exhibits Zn^{2+}-dependent cytotoxicity. The previous study lacks the information on the effect of zinc on cell lethality caused by Ziram, the mechanism of the action of sublethal levels of Ziram in the presence of environmentally relevant levels of zinc, and its implication in toxicological and environmental sciences.

Zinc is used in many industries, and the industrial wastewater is polluted with the excessive amount of zinc released [7]. The maximum zinc concentration in river water ranged from 0.14 to 0.22 mg/L in the rivers of north Portugal [8], and from 0.08 to 1.76 mg/L in the Gombak and Penchala Rivers, Malaysia [9]. Zinc concentration in water samples collected from the Godavari River, India, ranged from 4.2 to 6.7 mg/L [10]. The calculated zinc concentrations in samples collected from these rivers were 2.1–102.4 μM. Therefore, the concentration of zinc in river water may be critical for the evaluation of environmental toxicity of Ziram.

In this study to test the hypothesis described above, we have cytometrically examined the effects of sublethal levels of Ziram on rat thymic lymphocytes in the presence of zinc at environmentally relevant levels. This study may provide basic information regarding the mechanisms underlying Zn^{2+}-related adverse actions caused by Ziram at sublethal levels on wild mammals.

2. Materials and methods

2.1. Chemicals

Ziram (purity 99.9%) was a product of Tokyo Chemical Industry Co., Ltd. (Tokyo, Japan). Chemical structure of Ziram is shown in Fig. 1. Fluorescent probes described below were purchased from Invitrogen (Eugene, OR, USA). The Zn^{2+} chelators for extracellular and intracellular Zn^{2+}, diethylenetriamine-N,N,N′,N″,N″-pentaacetic acid and N,N,N′,N′-tetrakis(2-pyridylmethyl)ethylenediamine (DTPA and TPEN, respectively), were purchased from Dojindo Molecular Technologies, Inc. (Kumamoto, Japan). Other chemicals were purchased from Wako Pure Chemicals (Osaka, Japan) unless mentioned otherwise.

(Figure 1 near here)

2.2. Animals and cell preparation

Animal experiments were performed under the approval (No. 05279) by the Committee for Animal Experiments at the University of Tokushima.

Thymus glands were obtained from rats that were anesthetized with ether. To dissociate thymocytes, the sliced glands were triturated in chilled Tyrode's solution (2–4 °C). The pH of Tyrode's solution was adjusted at 7.4 by 5 mM 4-(2-hydroxyethyl)-1-piperazineethanesulfonic acid and appropriate amount of NaOH. The cell suspension was incubated at 36–37 °C for 1 h before the experiments. It is noted that the suspension contained trace amounts (216.9 ± 14.4 nM) of zinc from cell preparation [11]. Thymocytes are employed for this model experiment of cytotoxicity caused by chemical reagents because of following reasons. First, single dissociated cells with intact membranes are obtained because no enzymatic treatment was required to isolate single cells. Second, several types of chemical and biological substances cause cell death in thymocytes [12–14]. Third, the process of cell death (necrosis, apoptosis, and autophagy) in thymocytes is well studied [15–17].

Ziram (0.1–1 mM in 2 μL DMSO) and/or $ZnCl_2$ (0.1–10 mM in 2 μL distilled water) were applied to 2 mL of suspensions in test tubes and incubated at 36–37°C for 2–4 h. A sample (100 μL) from 2 mL of each suspension was cytometrically analyzed by a flow cytometry. The

data acquisition time for 2500 cells per one measurement was 10–15 s.

2.3. Fluorescence measurements of cellular parameters

To estimate lethality of rat thymocytes, 5 μM propidium iodide was added to the cell suspension because propidium stains dead cells and cells with compromised membranes. The superoxide anions in the cells were detected using 5 μM hydroethidine [18]. The cells were treated with hydroethidine for 30 min and then test agents were added to the cell suspension. The cellular content of glutathione was estimated with 5-chloromethylfluorescein diacetate (5-CMF-DA) [19]. The cells were incubated with 5-CMF-DA for 30 min before the measurement of 5-CMF fluorescence.

The fluorescence as membrane and intracellular parameters were measured from the cells using a flow cytometer (CytoACE-150; JASCO, Tokyo, Japan) with the software (Version 3.06; JASCO). Excitation wavelength of argon laser was 488 nM. Emissions from the cells were detected at 530 ± 20 nm (green fluorescence) for 5-CMF fluorescence and at 600 ± 20 nm (red fluorescence) for propidium and ethidium fluorescence. 5-CMF fluorescence was monitored in living cells without propidium fluorescence. No fluorescence from chemical reagents except for fluorescent dyes was detected under present experimental conditions.

2.4. WST assay

Cells were incubated with the WST-1 reagent (Dojindo Molecular Technologies, Inc., Kumamoto, Japan) for 2 h in a 96-well tissue culture plate after the cells were co-treated with 0.3 μM Ziram and 10 μM $ZnCl_2$ for 3 h. Thereafter, the formation of formazan was quantitated with a microplate reader (MTP-310Lab, Corona Electric, Hitachinaka, Japan). The measured absorbance at 450 nm correlates with the number of viable cells.

2.5. Statistical test and data representation

Statistical tests were conducted using ANOVA with Tukey's multivariate analysis. P-values of < 0.05 were considered significant. Results were expressed as mean and standard deviation of 4–8 samples. Each series of experiments was repeated three times unless specified

otherwise.

3. Results

3.1. Ziram-induced increase in cell lethality

The treatment of rat thymocytes with 1 μM Ziram for 4 h significantly increased the population of cells showing propidium fluorescence, indicating the increase in cell lethality by Ziram (Fig. 2A). This Ziram action was associated with decrease in forward scatter intensity of living cells. The intensity decreased significantly from 152.2 ± 1.7 (mean ± S.D. of four samples) to 138.1 ± 0.7 in the presence of 1 μM Ziram, showing that Ziram induced cell shrinkage. This decrease was statistically significant ($P < 0.01$). Ziram at a concentration of 0.3 μM did not significantly increase the cell lethality (Fig. 2B). Therefore, 0.3 μM Ziram was considered as the threshold concentration under the present condition. However, 0.3 μM Ziram slightly increased side scatter, a parameter of cell density (Fig. 2C).

(Figure 2 near here)

3.2. Effects of Zn^{2+} chelators on Ziram-induced increase in cell lethality

Ziram increased intracellular Zn^{2+} concentration ($[Zn^{2+}]_i$) via Zn^{2+} influx [6]. We proposed that if Zn^{2+} was involved in Ziram-induced increase in lethality, the chelation of Zn^{2+} by using DTPA or TPEN would attenuate the cytotoxicity of Ziram. The treatment of cells with the Zn^{2+} chelators separately for 4 h did not change the cell lethality. Ziram at 1 μM did not increase cell lethality in the presence of the Zn^{2+} chelators (Fig. 3), suggesting the involvement of Zn^{2+} in Ziram-induced cytotoxicity.

(Figure 3 near here)

3.3. Effect of $ZnCl_2$ on cells treated with Ziram

Ziram at a sublethal concentration (0.3 μM), slightly but significantly, elevated $[Zn^{2+}]_i$, and the simultaneous application of Ziram and $ZnCl_2$ induced a further profound elevation of $[Zn^{2+}]_i$ [19]. We proposed that if the cytotoxicity of Ziram was dependent on Zn^{2+}, the combination

of Ziram and $ZnCl_2$ would have greatly increased the cell lethality. Ziram at a sublethal concentration of 0.3 μM greatly increased cell lethality in the presence of 10 μM $ZnCl_2$ (Fig. 4A). This was also observed in the case of 1 μM Ziram. These results suggest the Zn^{2+} dependence of Ziram cytotoxicity. The suggestion was supported by the results obtained with WST assay. As shown in Fig. 4B, the co-treatment of cells with 0.3 μM Ziram and 10 μM $ZnCl_2$ for 3 h significantly reduced the cell viability. Interesting phenomenon was observed in the living cells simultaneously treated with 0.3 μM Ziram and 10 μM $ZnCl_2$. There was a reduction of cell volume (cell shrinkage) of living cells co-treated with Ziram and $ZnCl_2$ (Fig. 4C). Cell shrinkage is known as one of parameters during an early stage of apoptosis [21].

(Figure 4 near here)

3.4. Zn^{2+}-dependent cytotoxicity of Ziram under cold conditions

The increase in $[Zn^{2+}]_i$ induced by treatment with $ZnCl_2$ or Ziram or both was significantly attenuated under cold conditions (4°C). The increase in cell lethality by 1 μM Ziram with and without 10 μM $ZnCl_2$ was completely suppressed under cold conditions (Fig. 5). These findings showed that the Zn^{2+}-dependent cytotoxicity of Ziram was completely inhibited under cold conditions.

(Figure 5 near here)

3.5. Changes in cellular content of GSH induced by Ziram, $ZnCl_2$, and their combination

The treatment of cells with $ZnCl_2$ increased the cellular content of GSH via an elevation in $[Zn^{2+}]_i$ [20]. The treatment of cells with 10 μM $ZnCl_2$ for 2 h increased the intensity of 5-CMF fluorescence whereas treatment with 0.3 μM Ziram did not increase the intensity (Fig. 6). The simultaneous treatment of cells with 0.3 μM Ziram and 10 μM $ZnCl_2$ for 2 h significantly attenuated 5-CMF fluorescence (Fig. 6). Thus, the combination of Ziram and $ZnCl_2$ induced the depletion of cellular GSH.

(Figure 6 near here)

3.6. Effects of Ziram, $ZnCl_2$, and their combination on production of superoxide anions

The effect of simultaneous application of 0.3 μM Ziram and 10 μM $ZnCl_2$ on oxidative stress is depicted in Fig. 6. Hydroethidine upon reaction with cellular superoxide anions forms ethidium that intercalates with DNA. The treatment of cells separately with either Ziram or $ZnCl_2$ for 2 h did not increase the ethidium fluorescence (Fig. 7). When the cells were simultaneously treated with 0.3 μM Ziram and 10 μM $ZnCl_2$ for 2 h, the intensity of ethidium fluorescence significantly augmented (Fig. 7). Thus, it is likely that the simultaneous treatment with Ziram and $ZnCl_2$ produced an excessive increase in the cellular content of superoxide anions.

(Figure 7 near here)

4. Discussion

4.1. Zn^{2+}-dependent cytotoxicity of Ziram

Ziram increased $[Ca^{2+}]_i$ in neuronal cells [22]. This was reminiscent of the possibility that Ziram induced a nonspecific increase in membrane permeability because it also increased $[Zn^{2+}]_i$ [19]. However, the augmentation of Fluo-3 fluorescence, an indicator of intracellular Ca^{2+}, by Ziram was not observed in the presence of TPEN, a chelator of intracellular Zn^{2+}. Thus, Ziram specifically increases membrane Zn^{2+} permeability in rat thymocytes.

The graphs in Figs. 2 and 3 clearly show that the cytotoxicity of Ziram is Zn^{2+}-dependent. We observed that Ziram increased $[Zn^{2+}]_i$ by increasing Zn^{2+} influx in rat thymocytes [19],. Although the application of $ZnCl_2$ further augmented the Ziram-induced elevation of Zn^{2+}, the chelation of external Zn^{2+} by DTPA attenuated it. The changes in cell lethality induced by Ziram (Figs. 2 and 3) seemed to be synchronized with the changes in $[Zn^{2+}]_i$ induced by Ziram when the cells were simultaneously treated with $ZnCl_2$ or DTPA. The increase in $[Zn^{2+}]_i$ by Ziram and $ZnCl_2$ was significantly attenuated under cold conditions. Thus, the Ziram-induced cytotoxicity was also attenuated under cold conditions (Fig. 5), supporting the suggestion that the cytotoxicity of Ziram is Zn^{2+}-dependent.

Simultaneous treatment with 0.3 μM Ziram and 10 μM $ZnCl_2$ greatly decreased the cellular GSH content, whereas treatment with $ZnCl_2$ alone increased the cellular GSH content and treatment with Ziram alone did not cause any change (Fig. 6). The superoxide anion content in cells simultaneously treated with 0.3 μM Ziram and 10 μM $ZnCl_2$ significantly increased, whereas it did not increase when the cells were treated with either Ziram or $ZnCl_2$ (Fig. 7). The simultaneous treatment with 0.3 μM Ziram and 10 μM $ZnCl_2$ induced an excessive elevation of $[Zn^{2+}]_i$ [19]. Excessive elevation of $[Zn^{2+}]_i$ was reported to induce oxidative stress or increase the vulnerability to oxidative stress or both [23–25]. Thus, it was considered that the increase in the cellular content of superoxide anions induced by the treatment with of Ziram and $ZnCl_2$ induced oxidative stress that decreased cellular GSH content.

4.2. Implication

Ziram protects plants from fungal infection [1,2,26]. The use of Ziram has expanded because of its utility as an antifouling agent [27]. Therefore, the environmental and health risk associated with Ziram use is of concern [2,3]. As Zn^{2+} potentiates the cytotoxicity of Ziram as described in this study, the environmental level of Zn^{2+} is critical for the evaluation of the environmental toxicity of Ziram. Zinc is widely used in many industries, and the wastewater from these industries is polluted with the excessive amount of zinc discharged through the waste [7]. The concentration of zinc varies among rivers. The calculated zinc concentrations in samples collected from the polluted rivers were 2.1–102.4 μM as described in the Introduction. Since the concentration of $ZnCl_2$ used in this study was 10 μM, equivalent to 0.65 mg/L of Zinc, it may be considered that the zinc concentration of samples collected from some testing points of rivers affected the toxicity of Ziram. Therefore, the environmental zinc level is important to evaluate the toxicity of Ziram to wild animals. The Zn^{2+}-induced potentiation of cytotoxicity is not specific for Ziram because the simultaneous application of $ZnCl_2$ also augmented the cytotoxicity of imidazole antifungals [28].

According to the Pesticide Effects Determination reported from Environmental Fate and

Effects Division, Office of Pesticide Programs (Washington DC, USA) [29], estimated aquatic peak concentrations of Ziram in surface water near Californian farms, USA were 9.89-43.7 μg/L (0.032-0.142 μM). Under *in vitro* conditions, the co-treatment of cells with 0.3 μM Ziram and 10 μM $ZnCl_2$ greatly increased cell lethality. If Ziram is absorbed and accumulated in wild animals, the toxicity of Ziram would be dependent on the extracellular Zn^{2+} concentration.

Conflict of interest

All authors affirm that there are no conflicts of interest to declare.

Founding source / Acknowledgement

This study was supported by a Grant-in-Aid for Scientific Research (C26340039) from the Japan Society for the Promotion of Science (Tokyo, Japan).

References

1 H. Berrada, M. Fernández, M.J. Ruiz, J.C. Moltó, J. Mañes, G. Font, G., Surveillance of pesticide residues in fruits from Valencia during twenty months (2004/05), Food Control 21(1) (2010) 36–44.

2 I.N. Tsakiris, M. Toutoudaki, M. Kokkinakis, M. Paraskevi, A.M. Tsatsakis, A.M., A risk assessment study of Greek population dietary chronic exposure to pesticide residues in fruits, vegetables and olive oil. Pesticides-formulations, effects, fate. Stoytcheva, M. (Ed.). InTech, (2011) 253–268.

3 B. Lozowicka, Health risk for children and adults consuming apples with pesticide residue, Sci. Total Environ. 502 (2015) 184–198.

4 A.M. Matei, L.D. Trombetta, L.D., Exposure of rat hippocampal astrocytes to Ziram increases oxidative stress. Toxicol. Ind. Health 5(2013) 0748233713504809.

5 W. Maret, W., Oxidative metal release from metallothionein via zinc-thiol/disulfide interchange, Proc. Natl. Acad. Sci. USA. 91(1) (1994) 237–241.

6 Y. Kanemoto-Kataoka, T.M. Oyama, H. Ishibashi, Y. Oyama, Y., Dithiocarbamate fungicides increase intracellular Zn^{2+} levels by increasing influx of Zn^{2+} in rat thymic lymphocytes, Chem. Biol. Interact. 237 (2015) 80–86.

7 C. Gakwisiri, N. Raut, A. Al-Saadi, S. Al-Aisri, A, Al-Ajmi, A critical review of removal of zinc from wastewater, Proc. World Cong. Eng. 1 (2012) 627–630.

8 A.I. Gomes, J.C. Pires, S.A. Figueiredo, R.A. Boaventura, Optimization of river water quality surveys by multivariate analysis of physicochemical, bacteriological and ecotoxicological data, Water Resour. Manag. 28(5) (2014) 1345–1361.

9 Z. Ismail, K. Salim, S.Z. Othman, A.H. Ramli, S.M. Shirazi, R. Karim, S.Y. Khoo, Determining and comparing the levels of heavy metal concentrations in two selected urban river water, Measurement 46(10) (2013) 4135–4144.

10 J.A. Sayyed, A.B. Bhosle, The study of zinc metal concentration by spectrophotometric method from Godavari River at Nanded, Maharashatra, Der Chemica Sinica J. (Pelagia Res. Library) 1(2) (2010) 104–109.

11 Y. Sakanashi, T.M. Oyama, Y. Matsuo, T.B. Oyama, Y. Nishimura, S. Ishida, S. Imai, Y. Okano, Y. Oyama, Zn^{2+}, derived from cell preparation, partly attenuates Ca^{2+}-dependent cell death induced by A23187, calcium ionophore, in rat thymocytes, Toxicol. In Vitro 23(2) (2009) 338–345.

12 E. Corsini, M. Sokooti, C.L. Galli, A. Moretto, C. Colosio, C., Pesticide induced immunotoxicity in humans: a comprehensive review of the existing evidence, Toxicology 307 (2013) 123–135.

13 L. Kuchler, L.K. Sha, A.K. Giegerich, T. Knape, A. Weigert, B. Brüne, A. Von Knethen, A., Sphingosine-1 phosphate promotes thymic atrophy during sepsis progression, Critical Care 18(S2) (2014) P51.

14 I. Solti, K. Kvell, G. Talaber, S. Veto, P. Acs, F. Gallyas Jr, Z. Illes, K. Fekete, P. Zalan, A. Szanto, Z. Bognar, Thymic atrophy and apoptosis of $CD4^+$ $CD8^+$ thymocytes in the cuprizone model of multiple sclerosis, PloS one 10(6) (2015) e0129217.

15 L. Klein, B. Kyewski, P.M. Allen, K.A. Hogquist, Positive and negative selection of the T cell repertoire: what thymocytes see (and don't see), Nature Rev. Immunol. 14(6) (2014) 377–391.

16 I.K. Poon, C.D. Lucas, A.G. Rossi, K.S. Ravichandran, Apoptotic cell clearance: basic biology and therapeutic potential, Nature Rev. Immunol. 14(3) (2014) 166–180.

17 S. Shimizu, T. Yoshida, M. Tsujioka, S. Arakawa, Autophagic cell death and cancer, Intl. J. Molec. Sci. 15(2) (2014) 3145–3153.

18 G. Rothe, G. Valet, Flow cytometric analysis of respiratory burst activity in phagocytes with hydroethidine and 2',7'-dichlorofluorescin, J. Leukoc. Biol. 47(5) (1990) 440–448.

19 L. Chikahisa, Y. Oyama, E. Okazaki, K. Noda, Fluorescent estimation of H_2O_2-induced

changes in cell viability and cellular nonprotein thiol level of dissociated rat thymocytes, Jpn J. Pharmacol. 71(4) (1996) 299–305.

20 A. Kinazaki, H. Chen, K., Koizumi, T. Kawanai, T.M. Oyama, M. Satoh, S. Ishida, Y. Okano, Y. Oyama, Putative role of intracellular Zn^{2+} release during oxidative stress: a trigger to restore cellular thiol content that is decreased by oxidative stress, J. Physiol. Sci. 61(5) (2011) 403–409.

21 E. Maeno, Y. Ishizaki, T. Kanaseki, A. Hazama, Y. Okada, Normotonic cell shrinkage because of disordered volume regulation is an early prerequisite to apoptosis. Proceedings of the National Academy of Sciences, 97(17) (2000) 9487–9492.

22 S.M. Han, K.J. Shin,Y.H. Kim, S.H. Kim, T. Lee, E. Kim, S.H. Ryu, P.G. Suh, Thiram and ziram stimulate non-selective cation channel and induce apoptosis in PC12 cells. NeuroToxicol. 24(3) (2003) 425–434.

23 S.L. Sensi, P. Paoletti, J.Y. Koh, E. Aizenman, A.L. Bush, M. Hershfinkel, The neurophysiology and pathology of brain zinc, J. Neurosci. 31(45) (2011) 16076–16085.

24 T.M. Oyama, M. Saito, T. Yonezawa, Y. Okano, Y. Oyama, Nanomolar concentrations of zinc pyrithione increase cell susceptibility to oxidative stress induced by hydrogen peroxide in rat thymocytes, Chemosphere 87(11) (2012) 1316–1322.

25 W. Wu, P.A. Bromberg, J.M. Samet, Zinc ions as effectors of environmental oxidative lung injury, Free Radic. Biol. Med. 65 (2013) 57–69.

26 O. López-Fernández, R. Rial-Otero, C. González-Barreiro, J. Simal-Gándara, Surveillance of fungicidal dithiocarbamate residues in fruits and vegetables, Food Chem. 134(1) (2012) 366–374.

27 N. Voulvoulis, M.D. Scrimshaw, J.M. Lester, Alternative antifouling biocides, Appl. Organomet. Chem. 13(3) (1999) 135–143.

28 H. Matsui, Y. Sakanashi, T.M. Oyama, Y. Oyama, S.I. Yokota, S. Ishida, Y. Okano, T.B. Oyama, Y. Nishimura, Imidazole antifungals, but not triazole antifungals, increase

membrane Zn^{2+} permeability in rat thymocytes: Possible contribution to their cytotoxicity, Toxicology 248(2) (2008) 142–150.

29 Environmental Fate and Effects Division, Office of Pesticide Programs, Risks of Ziram Use to Federally Threatened California Red-legged Frog (*Rana aurora draytonii*), Pesticide Effects Determination (2008) https://www3.epa.gov/pesticides/endanger/litstatus/effects/redleg-frog/ziram/determination.pdf

Figure legends

Fig. 1. Structure of Ziram.

Fig. 2. Change in cell lethality induced by Ziram. (A) Ziram-induced change represented in cytogram (propidium fluorescence versus forward scatter). The cytogram was constructed with 2500 cells. The dotted line under the cytogram indicates the population of cells exhibiting propidium fluorescence, dead cells, or the cells with compromised membranes. (B) Concentration-dependent change in cell lethality induced by Ziram. (C) Concentration-dependent change in side scatter intensity induced by Ziram. Column and bar depict the mean value and standard deviation of four samples, respectively. Asterisks (**) indicate the significant differences ($P < 0.01$) between the control group (CONTROL) and the group of cells treated with Ziram.

Fig. 3. Effects of Zn^{2+} chelators (DTPA and TPEN) on the cytotoxicity of Ziram. Column and bar depict the mean value and standard deviation of four samples, respectively. Asterisks (**) indicate the significant differences ($P < 0.01$) between the control group (CONTROL) and the group of cells treated with Ziram or respective Zn^{2+} chelator or both.

Fig. 4. Changes in the cytotoxicity of Ziram caused by $ZnCl_2$. (A) Increase in cell lethality by the co-treatment with Ziram and $ZnCl_2$. (B) Decrease in cell viability by the co-treatment with 0.3 μM Ziram and 10 μM $ZnCl_2$. Experiment was carried out with WST assay. (C) Reduction of cell volume ratio in the cells simultaneously treated with 0.3 μM Ziram and 10 μM $ZnCl_2$. Relative changes in cell volume were tentatively calculated by third power of mean cell size (relative intensity of forward scatter). Column and bar depict the mean value and standard deviation of four samples, respectively. Asterisks (**) indicate the significant differences ($P <$

0.01) between the control group (CONTROL) and the group of cells treated with Ziram or $ZnCl_2$ or both. Symbol (##) indicates the significant difference ($P < 0.01$) between the groups of cells treated with and without $ZnCl_2$.

Fig. 5. Cytotoxicity of Ziram under cold conditions. Column and bar depict the mean value and standard deviation of four samples, respectively. Asterisks (**) indicate the significant differences ($P < 0.01$) between the control group (CONTROL) and the group of cells treated with Ziram or $ZnCl_2$ or both. Symbol (##) indicates the significant difference ($P < 0.01$) between the groups of cells treated with and without $ZnCl_2$.

Fig. 6. Changes in the intensity of 5-CMF fluorescence by Ziram, $ZnCl_2$, and their combination. Column and bar depict the mean value and standard deviation of four samples, respectively. Asterisks (**) indicate the significant differences ($P < 0.01$) between the control group (CONTROL) and the group of cells treated with Ziram or the combination of Ziram and $ZnCl_2$. Symbol (##) indicates the significant difference ($P < 0.01$) between the group of cells treated simultaneously with Ziram and $ZnCl_2$ and other groups.

Fig. 7. Changes in the intensity of ethidium fluorescence by treatment with Ziram, $ZnCl_2$, and their combination. Column and bar depict the mean value and standard deviation of four samples, respectively. Asterisks (**) indicate the significant differences ($P < 0.01$) between the control group (CONTROL) and the group of cells treated with Ziram or the combination of Ziram and $ZnCl_2$. Symbol (##) indicates the significant difference ($P < 0.01$) between the group of cells simultaneously treated with Ziram and $ZnCl_2$ and other groups.

Figure 1

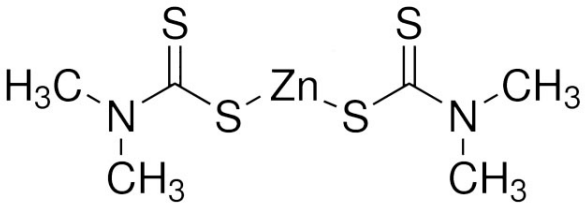

Figure 2

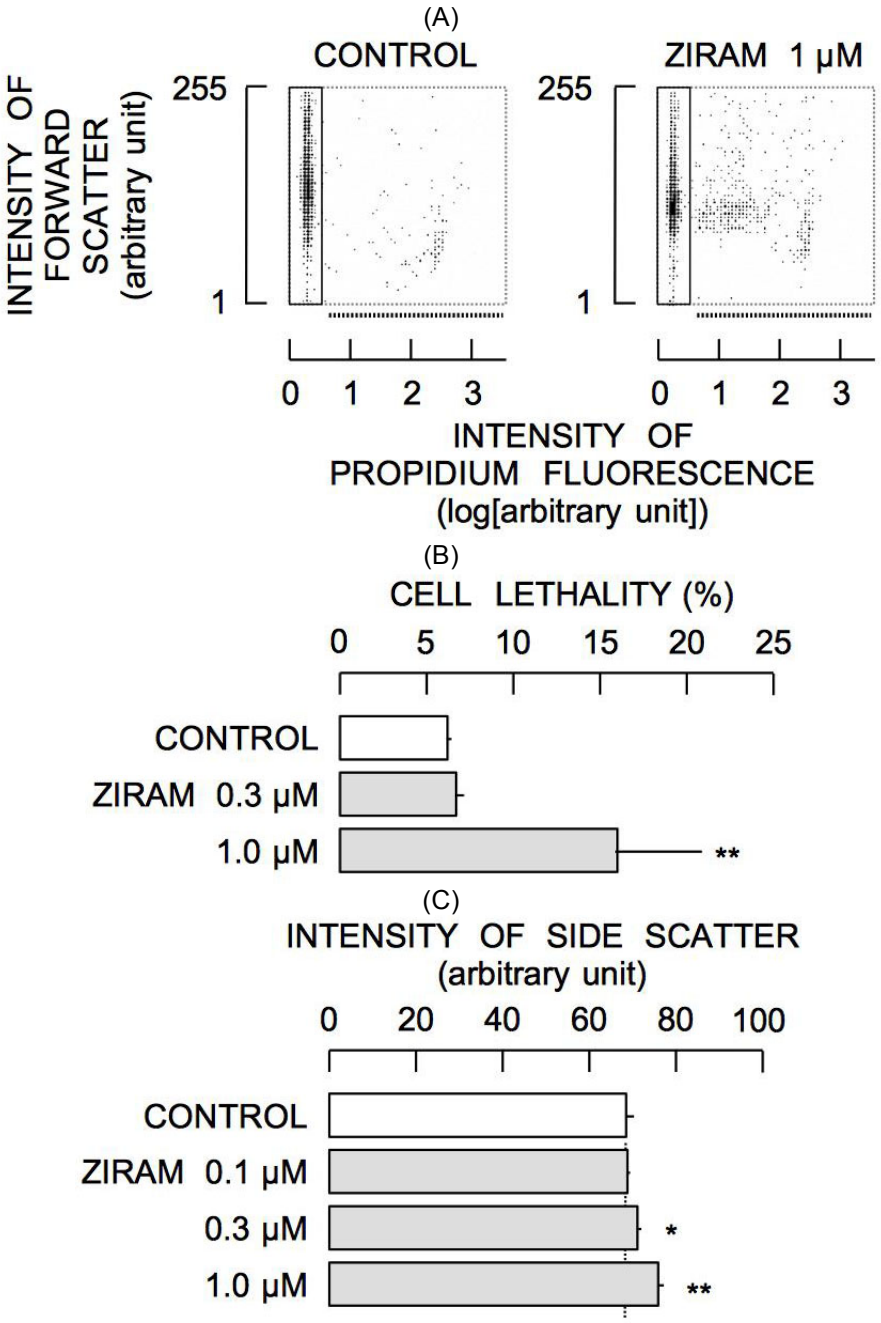
(A)
CONTROL
ZIRAM 1 μM
INTENSITY OF FORWARD SCATTER (arbitrary unit)
255
1
0 1 2 3
INTENSITY OF PROPIDIUM FLUORESCENCE (log[arbitrary unit])
(B)
CELL LETHALITY (%)
0 5 10 15 20 25
CONTROL
ZIRAM 0.3 μM
1.0 μM
**
(C)
INTENSITY OF SIDE SCATTER (arbitrary unit)
0 20 40 60 80 100
CONTROL
ZIRAM 0.1 μM
0.3 μM
1.0 μM
*
**

Figure 3

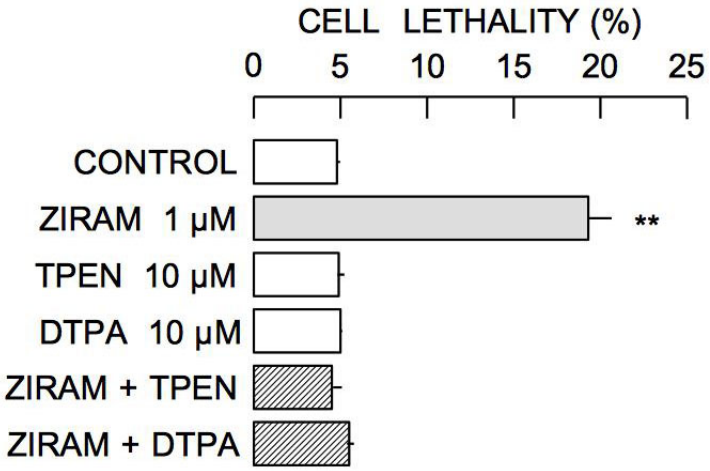
CELL LETHALITY (%)
0
5
10
15
20
25
CONTROL
ZIRAM 1 μM
**
TPEN 10 μM
DTPA 10 μM
ZIRAM + TPEN
ZIRAM + DTPA

Figure 4

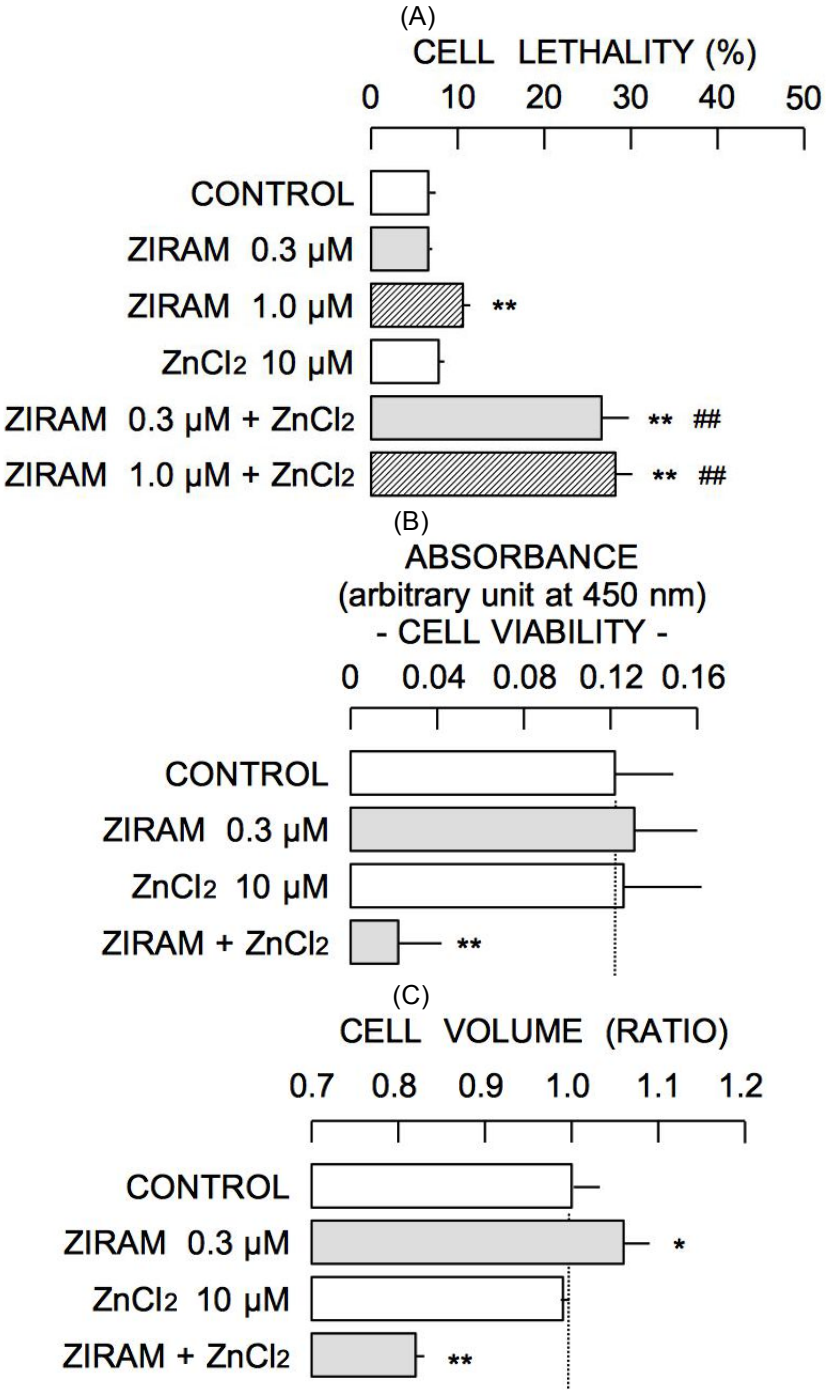
(A)
CELL LETHALITY (%)
0 10 20 30 40 50
CONTROL
ZIRAM 0.3 μM
ZIRAM 1.0 μM **
ZnCl2 10 μM
ZIRAM 0.3 μM + ZnCl2 ** ##
ZIRAM 1.0 μM + ZnCl2 ** ##
(B)
ABSORBANCE
(arbitrary unit at 450 nm)
- CELL VIABILITY -
0 0.04 0.08 0.12 0.16
CONTROL
ZIRAM 0.3 μM
ZnCl2 10 μM
ZIRAM + ZnCl2 **
(C)
CELL VOLUME (RATIO)
0.7 0.8 0.9 1.0 1.1 1.2
CONTROL
ZIRAM 0.3 μM *
ZnCl2 10 μM
ZIRAM + ZnCl2 **

Figure 5

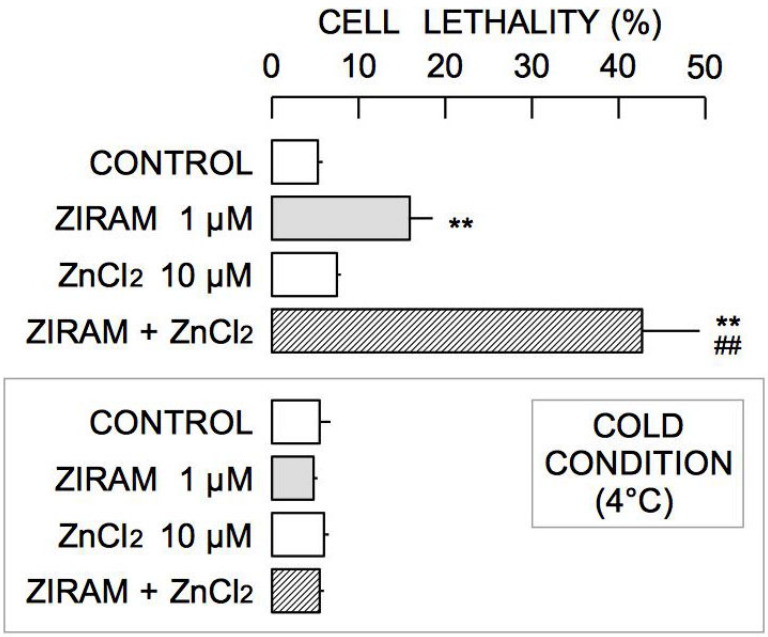
CELL LETHALITY (%)
0
10
20
30
40
50
CONTROL
ZIRAM 1 μM
**
ZnCl2 10 μM
ZIRAM + ZnCl2
**
##
CONTROL
ZIRAM 1 μM
ZnCl2 10 μM
ZIRAM + ZnCl2
COLD CONDITION (4°C)

Figure 6

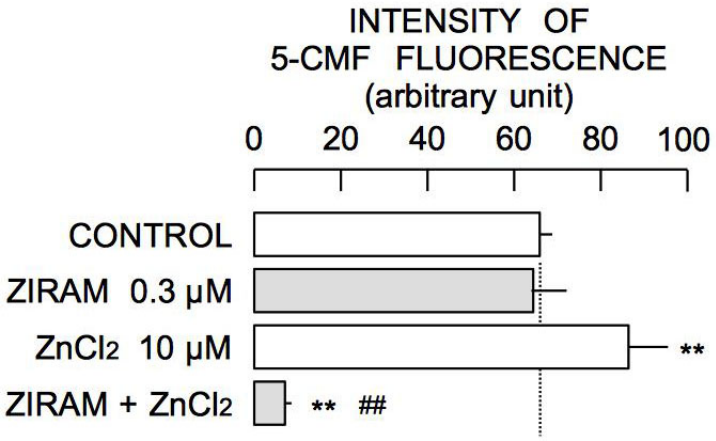
INTENSITY OF
5-CMF FLUORESCENCE
(arbitrary unit)
0
20
40
60
80
100
CONTROL
ZIRAM 0.3 µM
ZnCl2 10 µM
ZIRAM + ZnCl2
**
** ##

Figure 7

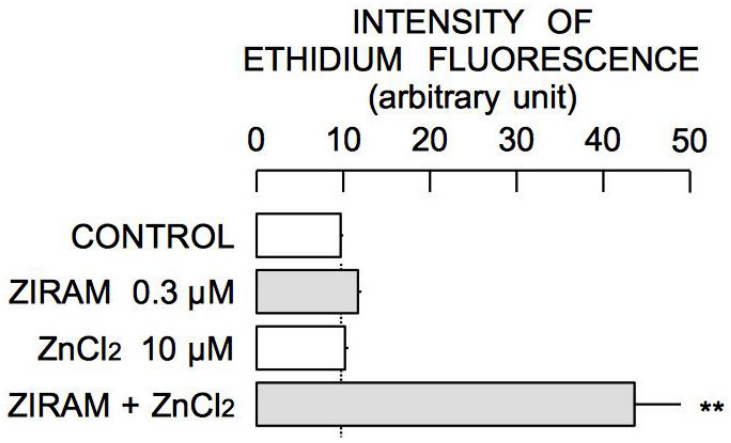
INTENSITY OF
ETHIDIUM FLUORESCENCE
(arbitrary unit)
0
10
20
30
40
50
CONTROL
ZIRAM 0.3 µM
ZnCl2 10 µM
ZIRAM + ZnCl2
**